Biophysical Chemistry, 45 (1992) 133–141
Elsevier Science Publishers B.V., Amsterdam

BIOCHE 01704

Distance distribution in a dye-linked oligonucleotide determined by time-resolved fluorescence energy transfer

Remo A. Hochstrasser, Shiow-Meei Chen and David P. Millar

The Scripps Research Institute, Department of Molecular Biology, MB20, 10666 N. Torrey Pines Road, La Jolla, CA 92037 (USA)

(Received 1 June 1992; accepted 9 July 1992)

Abstract

Fluorescence energy transfer is potentially a useful technique for obtaining structural and dynamic information on duplex and branched DNA molecules suitably labeled with donor and acceptor dyes. We have assessed the accuracy and limitations of FET measurements in nucleic acids with respect to the localization of the dyes and the flexibility of the dye–DNA linkages. A nine base-pair duplex oligonucleotide was synthesized with donor and acceptor dyes linked at the opposing 5′ termini by alkyl chains. A careful analysis of the fluorescence decay of the donor revealed that the donor–acceptor distance in this molecule was not well defined, but was described by a rather broad distribution. The mean donor–acceptor distance and the distribution of distances have been recovered from the donor decay. Orientational effects on energy transfer have been included in the analysis. The implications of these findings for FET measurements in nucleic acids are considered.

Keywords: Distance distribution; Fluorescence energy transfer; Time-resolved fluorescence spectroscopy; Fluorescent labeling; Synthetic oligonucleotides

1. Introduction

Fluorescence energy transfer (FET) has been widely used to determine proximity relationships in biological macromolecules, particularly in polypeptides and proteins [1]. Application of FET to nucleic acids has been limited by the difficulty of site-specific labeling with fluorophores. A notable exception are certain tRNA molecules that contain special bases which are naturally fluorescent or can be used as labeling sites [2,3]. However, FET studies of DNA have utilized non-specifically bound fluorophores, such as intercalators or groove-binders [4–6]. The structural information that can be obtained with these probes is limited by their lack of spatial localization at a unique position. The advent of automated oligonucleotide synthesis provides a general approach to site-specific fluorescent labeling of DNA. Using standard phosphoramidite chemistry, it is straightforward to synthesize an oligonucleotide containing an amine-reactive

Correspondence to: D.P. Millar, The Scripps Research Institute, Department of Molecular Biology, MB20, 10666 N. Torrey Pines Road, La Jolla, CA 92037 (USA)

linker at any desired position in the sequence [7–9]. The amine moiety can be readily labeled with a variety of fluorescent dyes and the resultant oligonucleotide-dye conjugates can be easily purified. As a result of these advances, it is expected that FET measurements in DNA will become more widespread and will yield more precise structural information than in the past.

This approach has been recently applied to both duplex [10,11] and branched [12] nucleic acid species labeled at the 5′ termini with dyes. A potential complication in the interpretation of FET measurements in these molecules is that the donor-acceptor distance may not be a consant, well defined quantity, owing to the flexibility of the alkyl chains used to link the dyes to the oligonucleotides. The usual relationship between the energy transfer efficiency and the sixth power of the donor–acceptor distance does not hold if a broad distribution of distances is present [13]. In addition to the flexibility of the dye–DNA linkages, the intrinsic flexibility of the nucleic acid structure could also influence the distribution of donor-acceptor distances. To establish that a range of donor–acceptor distances does actually exist in these molecules, the excited-state decay of the donor should be measured. Both time-resolved [14,15] and frequency domain [16] fluorescence methods have been used to determine the distribution of donor-acceptor distances in flexible bichromophoric molecules [17], oligopeptides [14] and proteins [15,18,19].

In this study, we have used time-resolved fluorescence spectroscopy to measure the decay of the donor excited-state in a nine base-pair duplex oligonucleotide containing donor and acceptor dyes linked to the opposing 5′ termini by hexyl chains. Analysis of the donor decay with models based on either a fixed donor–acceptor distance or a gaussian distribution of distances shows that a range of donor–acceptor distances does indeed exist in this dye-labeled DNA duplex. The mean donor–acceptor distance and the distribution of distances have been determined, taking into account orientational effects on energy transfer. The implications of these findings for FET measurements in DNA using 5′ linked dyes are discussed.

2. Materials and methods

2.1 Synthesis of 5′ amino oligonucleotides

Oligonucleotides were synthesized on an automated DNA synthesizer (Applied Biosystems model 108B) using beta cyanoethyl phosphoramidite derivatives. An aminohexyl phosphate linker was added to the 5′ terminus of the oligonucleotide using the aminolink-2 phosphoramidite (Applied Biosystems) during the final synthesis cycle. After standard cleavage and deprotection steps, the resulting oligonucleotides were purified by electrophoresis through denaturing urea acrylamide gels. Two complementary 5′ amino oligonucleotides were synthesized: strand 1 = (5′) TGAGGCCTA (3′), strand 2 = (5′) TAGGCCTCA (3′).

2.2 Dye labeling

Strand 1 was labeled with fluorescein and strand 2 was labeled with tetramethyl rhodamine, as follows. The 5′ amino oligonucleotides were incubated overnight at room temperature with a 200-fold molar excess of the *N*-hydroxyl succinimidyl dye ester (Applied Biosystems) in 20 m*M* sodium carbonate/bicarbonate buffer (pH 9.0). Unreacted dye esters were removed by size exclusion chromatography on a Sephedex G-25 column. Unlabeled oligonucleotides were removed by affinity chromatography using OPC cartridges (Applied Biosystems). The concentrations of the oligonucleotides were estimated from the 260 nm and visible absorbances (495 nm for fluorescein and 555 nm for tetramethyl rhodamine).

2.3 Duplex formation

Three different duplexes were used in the experiments: strand 1 labeled with fluorescein and strand 2 unlabeled (designated 1F:2U); strand 1 unlabeled and strand 2 labeled with tetramethyl rhodamine (1U:2R); strand 1 labeled with fluorescein and strand 2 labeled with tetramethyl rhodamine (1F:2R). These were prepared by annealing a mixture of the appropriate dye-labeled and/or unlabeled strands in 50 m*M* phosphate

buffer, pH 7.4, containing 0.15 *M* NaCl. No difference was found by annealing the samples at either 60°C or 20°C. The latter temperature was used in all cases. To ensure that the dye-labeled strand of interest was fully hybridized in each case, increasing amounts of the complementary strand were added and the fluorescence decay and time-dependent depolarization of the dye were measured. The dye-labeled strand was considered to be fully hybridized when these data did not change upon further addition of the complementary strand. This point was reached when approximately 1.0 molar equivalents of the complementary strand had been added. The 1F:2U and 1F:2R samples contained 2.0 equivalents of strand 2, and 1U:2R sample contained 2.0 equivalents of strand 1.

2.4 Time-resolved fluorescence spectroscopy

Samples were excited at 515 nm with the vertically polarized output of a mode-locked argon ion laser (Coherent Innova 100-12). The pulse duration was 90 ps. The pulse repetition frequency was reduced from 78 MHz to 1.87 MHz with an acousto-optic beam deflector placed outside the laser cavity. The fluorescence was collected at 90° to the excitation beam, passed through a polarizer and then focused on the slits of a 0.1m single grating monochromator (JY H-10). Measurements were made at either 530 nm (fluorescein dye) or 580 nm (tetramethyl rhodamine dye) with a spectral bandpass of 4 nm. A microchannel plate photomultiplier (Hamamatsu R2809U-01) placed at the exit slit of the monochromator was used to detect the fluorescence and its output was processed with a time-correlated single photon counting system. The instrument response function was measured by scattering the laser pulses into the detector with a dilute solution of non-dairy coffee creamer. The FWHM of the response was 100 ps. Between 10,000 and 100,000 single photon counts were accumulated in the peak channel of the fluorescence decay curve.

Isotropic fluorescence decay curves were measured with the emission polarizer oriented at 54.7° to the vertical excitation polarization. Time-dependent fluorescence depolarization was measured by alternating the emission polarizer between vertical and horizontal orientations every fifteen seconds and collecting the two decay curves in separate memory segments of a multichannel analyzer. The small polarization bias of the detection system was corrected for by multiplying the perpendicular polarized fluorescence intensity by 1.023 (g-factor). All measurements were made at 4°C.

2.5 Data analysis

The fluorescence decay of the donor in the absence of energy transfer is given by

$$I_D(t) = g(t) * K(t) \tag{1}$$

and

$$K(t) = \sum_{i=1}^{N} \alpha_i \exp(-t/\tau_i), \tag{2}$$

where $I_D(t)$ is the isotropic fluorescence decay of the donor in the absence of the acceptor, $g(t)$ is the instrument response function, $*$ denotes convolution of two functions, α_i is the fractional amplitude associated with each donor lifetime τ_i and N is the number of lifetimes. The parameters α_i and τ_i were optimized for a best-fit of eqs. (1) and (2) using a non-linear least-squares method [20]. The goodness of fit was judged by the reduced chi-square value, χ_r^2, and by examination of the weighted residuals [20].

The fluorescence decay of the donor in the presence of an acceptor at a fixed distance R is given by

$$I_{DA}(t) = g(t) * \left[(1-f) \sum_i \alpha_i \exp\left\{ (-t/\tau_i) \times \left[1 + (R_0/R)^6 \right] \right\} \right] + f I_D(t) \tag{3}$$

where $I_{DA}(t)$ is the donor decay in the presence of the acceptor and R_0 is the critical transfer distance. Note that α_i and τ_i are determined from eqs. (1) and (2). The first term describes the decay of donors that undergo energy transfer to the acceptor, while the second term accounts for a fraction (f) of donors that do not undergo

energy transfer. The critical transfer distance is determined by the spectral properties of the donor and acceptor

$$R_0^6 = \{9000(\ln 10)\kappa^2\phi_D/128\pi^5 N n^4\} \times \int_0^\infty F_D(\lambda)\epsilon_A(\lambda)\lambda^4 \, d\lambda \quad (4)$$

where κ^2 is an orientation factor, ϕ_D is the donor's fluorescence quantum yield, N is Avogadro's number, n is the refractive index of the medium separating the donor and acceptor, $F_D(\lambda)$ is the donor fluorescence intensity at wavelength λ and $\epsilon_A(\lambda)$ is the extinction coefficient of the acceptor at the same wavelength. The critical transfer distance for the fluorescein–tetramethyl rhodamine pair linked by a hydrocarbon chain is 54 Å (assuming $\kappa^2 = 2/3$) [21]. We assumed that this value could also be used for the dyes linked by an oligonucleotide chain.

If the donor–acceptor distance is instead described by a probability distribution, $P(R)$, then the donor decay is given by

$$I_{DA}(t) = g(t) * \left[(1-f) \int_0^\infty \sum_i \alpha_i \exp\left\{ (-t/\tau_i) \times \left[1 + (R_0/R)^6 \right] \right\} P(R) \, dR \right] + fI_D(t) \quad (5)$$

This equation assumes that the distribution of distances is static on the time scale of the energy transfer. We further assume $P(R)$ to be of gaussian shape:

$$P(R) = (\sigma\sqrt{2\pi})^{-1} \exp\left\{ -\frac{(R-\bar{R})^2}{2\sigma^2} \right\} \quad (6)$$

where $\bar{R}$ is the mean donor–acceptor distance and σ is the standard deviation of the distribution. The width of the distribution (FWHM) is given by 2.35σ.

The orientational dependence of the energy transfer process also influences the donor decay. If the donor and acceptor rotate freely on a time scale that is rapid compared with energy transfer, then eq. (5) is appropriate and R_0 is calculated with $\kappa^2 = \frac{2}{3}$. However, the rotation of the donor and acceptor dyes linked to DNA is hindered and κ^2 can have a range of values. The limiting values, κ_1^2 and κ_2^2, that were compatible with the rotational mobility of the dyes was estimated from the theory of Haas et al. [22]. The donor decay in eq. (5) was then averaged over this range of κ^2 values [15]

$$I_{DA}(t) = g(t) * \left[\frac{(1-f)}{(\beta_2 - \beta_1)} \int_{\beta_1}^{\beta_2} \int_0^\infty \sum_i \alpha_i \times \exp\left\{ -(t/\tau_i)\left[1 + (\beta R_0/R)^6 \right] \right\} \times P(R) \, dR \, d\beta \right] + fI_D(t) \quad (7)$$

where $\beta = \frac{3}{2}\kappa^2$. Note that R_0 is calculated with $\kappa^2 = \frac{2}{3}$, and that β corrects the value of R_0^6 in eq. (7). β_1 and β_2 correspond to κ_1^2 and κ_2^2, respectively.

Time-dependent fluorescence depolarization was used to determine the rotational mobility of the dyes. the data were analyzed according to the following equations:

$$I_\parallel(t) = g(t) * [\{1 + 2r(t)\}K(t)] \quad (8)$$

and

$$I_\perp(t) = g(t) * [\{1 - r(t)\}K(t)], \quad (9)$$

where

$$r(t) = \sum_{k=1}^{2} r_{0k} \exp(-t/\phi_k). \quad (10)$$

$I_\parallel(t)$ and $I_\perp(t)$ are the time-resolved intensities of the parallel and perpendicular polarization components of the fluorescence, $r(t)$ is the time-dependent fluorescence anisotropy and $K(t)$ is defined in eq. (2). In eq. (10), r_{01} and ϕ_1 are the limiting anisotropy and decay time associated with local rotation of the dye, while r_{02} and ϕ_2 are the corresponding quantities describing overall rotation of the dye-linked oligonucleotide. The total limiting anisotropy is $r_0 = r_{01} + r_{02}$. The parameters r_{0k} and ϕ_k were optimized for a simultaneous best fit to $I_\parallel(t)$ and $I_\perp(t)$ [23], with the parameters in the expression for $K(t)$ kept fixed

at the values determined from the isotropic fluorescence decay. The goodness of fit was judged as described above. The angular range of local dye rotation was estimated using a model for diffusion within a cone, with the cone semi-angle given by [24]

$$\theta = \cos^{-1}\left\{\tfrac{1}{2}\left[(1+8S)^{1/2}-1\right]\right\} \qquad (11)$$

where

$$S = (r_{02}/r_0)^{1/2}.$$

3. Results

3.1 Isolated donor decay

The fluorescence decay of the fluorescein donor was first measured in the duplex 1F:2U, in which the tetramethyl rhodamine acceptor was absent. Analysis of the isotropic decay of the fluorescein emission according to eqs. (1) and (2) indicated the presence of two lifetimes ($\chi_r^2 = 1.05$ with two lifetimes, $\chi_r^2 > 3$ with one lifetime). The best-fit parameter values are shown in Table 1. The decay was dominated by the 4.9 ns lifetime, which was similar to the lifetime of free fluorescein under the same conditions (data not shown). The minor lifetime was shorter than the free dye lifetime, indicating that some excited-state quenching occurred in the oligonucleotide-linked dye.

Table 1

Lifetime analysis of dye-linked duplexes [a]

Duplex [b]	λ_{em} (nm)	τ_1(ns) (±0.05)	τ_2(ns) (±0.10)	α_1 (±0.005)	α_2 (±0.005)
1F:2U	530	1.61	4.92	0.092	0.908
1U:2R	580	1.15	4.34	0.143	0.857

[a] λ_{ex} = 515 nm, 4°C.
[b] 1F:2U = F-(5′)TGAGGCCTA / ACTCCGGAT(5′) F = fluorescein
1U:2R = (5′)TGAGGCCTA / ACTCCGGAT(5′)-R R = tetramethyl rhodamine
The dye-labeled strands were hybridized with a two-fold excess of the unlabeled complementary oligonucleotide in each case. Standard errors of measurement are given in parentheses.

3.2 Rotational mobility of the donor and acceptor

Time-dependent fluorescence depolarization of duplexes 1F:2U and 1U:2R was used to determine the rotational mobility of the donor and acceptor dyes. Fluorescein emission was observed at 530 nm, while tetramethyl rhodamine emission was observed at 580 nm. The fluorescence depolarization data were analysed with eqs. (8) to (10). The dye lifetimes shown in Table 1 were used in the analyses. Excellent fits were obtained for both dyes ($\chi_r^2 = 1.05$). The best-fit parameter values are presented in Table 2.

Table 2

Anisotropy decay parameters [a]

Duplex [b]	λ_{em} (nm)	ϕ_1(ps) (±50)	ϕ_2(ns) (±0.15)	r_{01} (±0.005)	r_{02} (±0.005)	r_0 (±0.010)	θ(deg) [c] (±3)
1F:2U	530	241	4.61	0.116	0.253	0.369	28
1U:2R	580	323	4.57	0.169	0.168	0.337	38

[a] λ_{ex} = 515 nm, 4°C.
[b] 1F:2U = F-(5′)TGAGGCCTA / ACTCCGGAT(5′) F = fluorescein,
1U:2R = (5′)TGAGGCCTA / ACTCCGGAT(5′)-R R = tetramethyl rhodamine.
The dye-labeled strands were hybridized with a two-fold excess of the unlabeled complementary oligonucleotide in each case.
[c] Cone semi-angle calculated from eq. (11).
Standard errors of measurement are given in parentheses.

The longer anisotropy decay time (ϕ_2) was in the nanosecond range, as expected for rotational diffusion of the entire dye-linked oligonucleotide. In addition, the same decay time was obtained for both fluorescein and tetramethyl rhodamine dyes, which further confirms that ϕ_2 was due to overall motion of the duplex. The shorter decay time (ϕ_1) was in the picosecond range, reflecting the rapid local rotation of the dye. The cone semi-angle for local dye rotation, calculated from eq. (11), was 28° for fluorescein and 38° for tetramethyl rhodamine. These results indicate that both dyes underwent rapid, large amplitude rotational motions and that the rotation of fluorescein was somewhat more restricted than that of tetramethyl rhodamine.

The total limiting anisotropy, r_0, was in the range 0.34 to 0.37. This value was close to the theoretical maximum value of 0.4, showing that most of the anisotropy decay was resolved in the experiments. A fast decay of anisotropy may have been occurring within the 100 ps instrumental response time, but its amplitude must have been small.

A range of possible κ^2 values was estimated on the basis of these data. The limiting values, $\kappa_1^2 = 0.40$ and $\kappa_2^2 = 1.20$, encompass the most probable values of the orientation factor that are consistent with the rotational mobility of the dyes [22]. The corresponding β values, $\beta_1 = 0.6$ and $\beta_2 = 1.8$, were used as the limits of integration in eq. (7).

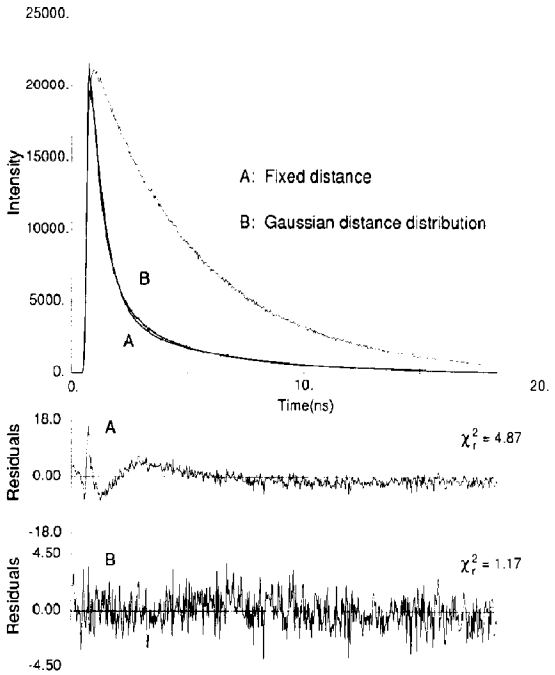

Fig. 1. Isotropic fluorescence decay of fluorescein in dye-labelled duplexes 1F:2U (upper curve) and 1F:2R (lower curve). The 1F:2U duplex was labeled with fluorescein at the 5′ terminus of strand 1, while strand 2 was unlabeled. The 1F:2R duplex was identical, except that strand 2 was labeled at the 5′ terminus with tetramethyl rhodamine. The base sequence of strands 1 and 2 are given in the text. The best fit of eqs. (3) and (5) are superimposed on the decay of 1F:2R and the weighted residuals for the two fits are shown below the decay. The χ_r^2 values for the two fits are also indicated. The fit to eq. (3), designated A, assumes a constant donor–acceptor distance. The fit to eq. (5), designated B, assumes a gaussian distribution of donor–acceptor distances. The corresponding best fit parameters in each case are given in Table 3.

3.3 Donor decay in the presence of the acceptor

Energy transfer was measured in the duplex 1F:2R, in which the fluorescein donor and tetramethyl rhodamine acceptor were located at opposing 5′ termini and separated by nine intervening base-pairs. The steady-state emission intensity of fluorescein was significantly reduced in 1F:2R compared with the same duplex lacking the acceptor dye, 1F:2U. The energy transfer efficiency calculated from the intensity reduction was 0.772.

The fluorescence decay of the fluorescein donor in 1F:2R was much more rapid than in 1F:2U (Fig. 1), again reflecting energy transfer from fluorescein to tetramethyl rhodamine. The donor decay was first analyzed with a fixed donor–acceptor distance. The best fit of eq. (3) was found by adjusting f and R using non-linear least squares. The parameters α_i and τ_i were kept fixed at the values determined in the absence of the acceptor (Table 1). The best fit curve is shown in Fig. 1 together with the weighted residuals. The corresponding parameter values are presented in Table 3. The fit was obviously poor, as indicated by the large χ_r^2 value and the systematic deviations apparent in the residuals (Fig. 1). We conclude that the donor decay in the

presence of the acceptor cannot be reproduced with a single donor–acceptor distance.

The donor decay was then analyzed with a gaussian distribution of distances according to eqs. (5) and (6). The integral in eq. (5) was evaluated numerically by Romberg integration [25]. The data were fitted by adjusting $\bar{R}$, σ and f using non-linear least squares. As shown in Fig. 1, the fit was clearly improved with a distribution of distances. This was also reflected in the χ_r^2 value. The best fit parameters are presented in Table 3.

Orientational effects on the donor decay were incorporated by averaging the donor decay function over the range of possible values for the orientation factor. The orientational average in eq. (7) was calculated numerically. The parameters $\bar{R}$, σ and f were again adjusted to achieve a best fit of eq. (7) to the donor decay curve in 1F:2R. The best fit parameters were almost identical to those obtained from eq. (5) (Table 3). The recovered distance distribution is shown in Fig. 2.

In the preceding analysis, it was assumed that R_0 was the same for both decay components of the donor, $i = 1$ and 2 in eqs. (3), (5) and (7). This is not strictly valid if the two decay components correspond to different configurations of the donor that do not interconvert during the excited-state lifetime [15]. However, the use of different R_0 values for each component, scaled according to the individual lifetimes [15], had no effect on the recovered parameters or the quality of the fits. This was not surprising since the isolated donor decay was not strongly heterogeneous (Table 1).

Table 3

Donor decay parameters in 1F:2R [a]

$\bar{R}$ (Å)	Width [b] (Å)	f [c]	β_1	β_2	χ_r^2
39.6 [d]	0	0.163	–	–	4.71
37.0 [e]	13.7	0.121	–	–	1.17
37.8 [f]	12.8	0.118	0.6	1.8	1.16

[a] 1F:2R = F-(5′)TGAGGCCTA / ACTCCGGAT(5′)-R F = fluorescein, R = tetramethyl rhodamine. Strand 2 was present in two-fold excess compared to strand 1. The sample temperature was 4°C.

[b] Full width at half maximum of the donor–acceptor distance distribution.

[c] Fraction of donors that do not transfer to an acceptor.

[d] Donor–acceptor distance determined from eq. (3).

[e] Mean donor–acceptor distance determined from eq. (5).

[f] Mean donor–acceptor distance determined from eq. (7).

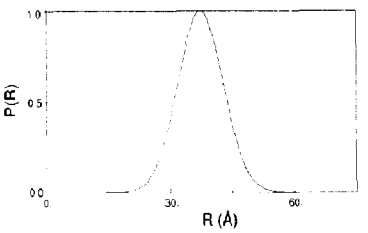

Fig. 2. Gaussian distribution of donor–acceptor distances in dye-labeled duplex 1F:2R determined from eq. (7).

The fits to eqs. (3), (5) or (7) all indicated that a small fraction (f) of the fluorescein donors in the 1F:2R sample did not undergo energy transfer to an acceptor (Table 3). Attempts to fit the donor decay with $f = 0$ in eqs. (3), (5) or (7) gave significantly worse fits in all cases. Nevertheless, even under these conditions, eqs. (5) and (7) still gave much better fits than eq. (3), again showing that a distribution of donor–acceptor distances was implied by the data. The presence of fluorescein donors that did not transfer to an acceptor could have been due to incomplete removal of unreacted fluorescein ester, incomplete removal of unlabeled strand 2, or incomplete hybridization of strands 1 and 2. Even with an efficiency of 97% at each of these steps, it is expected that 10% of the fluorescein dye in the 1F:2R sample will not be closely associated with an acceptor. This residual population of isolated donors is not a serious problem in time-resolved fluorescence measurements since they can be readily identified on the basis of their decay behaviour. However, in steady-state fluorescence measurements, these donor molecules are indistinguishable from those that do transfer to an acceptor, which leads to an underestimate of the transfer efficiency and an overestimate of the donor–acceptor distance. Based on intensity measurements alone, the transfer efficiency in 1F:2F was 0.772, which corresponds to an apparent donor–acceptor dis-

tance of 43.6 Å. This value is considerably larger than the true mean distance of 38 Å (Table 3).

4. Discussion

The existence of a range of donor–acceptor distances in the 1F:2R duplex is strongly implied by the donor decay analysis, but is also supported by other lines of evidence. Duplexes labeled with only the donor or acceptor dyes exhibited two fluorescence lifetimes, a long lifetime that was essentially identical to the free dye lifetime, and a shorter lifetime that indicated some degree of excited-state quenching. Since the shorter lifetime was absent in the free dye esters, it must have been due to an interaction between the dye and the oligonucleotide strand. We have previously shown that the magnitude of this short lifetime and its abundance depend strongly on the identity of the base at the 5′ end of the labeled strand, suggesting that the dye interacts closely with the DNA [26]. Therefore, the presence of both quenched and unquenched dye lifetimes implies the existence of a range of distances between the dyes and the 5′ termini of the oligonucleotides.

A Gaussian distribution of donor–acceptor distances that is consistent with the donor decay is shown in Fig. 2. A number of factors could contribute to the observed width of the distribution. (i) A range of orientations of the donor and acceptor transition dipoles. (ii) The hexyl chains linking the dyes to the 5′ phosphate group adopt a variety of conformations that place the dye at different distances from the DNA terminus. (iii) The bending flexibility of the double helix produces a distribution of end-to-end distances.

The contribution of orientational effects to the recovered distribution is minimal since both the donor and acceptor dyes rotate rapidly over a wide angular range, resulting in a substantial degree of dynamic averaging of the orientational dependence of the energy transfer rate. Thus the orientation factor κ^2 lies in a relatively narrow range about the limiting $\frac{2}{3}$ value. Averaging the donor decay function over this range of κ^2 values had only a minor effect on the recovered distribution parameters. The width of the recovered distribution therefore predominantly reflects a range of distances between the donor and acceptor dyes.

The hexyl chains that link the dyes to the 5′ phosphate group of each strand are flexible and could adopt a variety of conformations. As noted above, a range of distances between the dyes and the 5′ termini of the DNA is implied by the hetrogeneous decay of the isolated donor or acceptor dyes. Different conformations of the linker are presumably responsible for this behaviour. The linker flexibility is probably the major determinant of the donor–acceptor distance distribution in the 1F:2R duplex. The maximum distance between dyes should be about 57 Å, assuming that each extended linker adds 13 Å [10] to the length of the duplex (31 Å). This is consistent with Fig. 2.

The intrinsic flexibility of the DNA may also contribute to the width of the donor–acceptor distance distribution, although this is probably a small effect since the nine base-pair duplex is much shorter than the persistence length of double-helical DNA.

The analysis presented here assumes that the distance distribution is static on the time scale of the energy transfer. This assumption may not be strictly valid, since local conformational changes of the hexyl linker chains may occur in the subnanosecond time range. However, interconversion between compact folded conformations of the linker, that may be stabilized by dye–DNA interactions, and extended conformations that place the dye in solution is likely to occur on a much slower timescale than that of energy transfer. Treating the donor–acceptor distance distribution as static is therefore a reasonable first approximation. The effects of donor–acceptor diffusion can be included in a more sophisticated analysis [17].

5. Conclusions

Fluorescein and tetramethyl rhodamine dyes form a donor–acceptor pair with a large degree of spectral overlap and are consequently attrac-

tive for FET measurements of long range distances in nucleic acid molecules in solution. These dyes have been covalently linked to both duplex and branched DNA molecules by flexible alkyl chains [10–12]. The findings of this study show that caution must be used in interpreting energy transfer efficiencies in such labeled DNA molecules, since the donor–acceptor distance is described by a rather broad distribution that probably reflects the flexibility of the linkers. The usual relationship between the transfer efficiency and the sixth power of the donor–acceptor separation is not valid under these conditions. This may be responsible for the apparent failure of the Forster model to predict distances in a series of duplex oligonucleotides of different length [11]. In branched DNA molecules labeled at the branch termini with dyes [11,12], flexibility about the branch point will also contribute to the width of the donor-acceptor distance distribution. Time-resolved fluorescence energy transfer, combined with a distance distribution analysis, could provide information about the flexibility of such unusual nucleic acid structures.

6. Acknowledgements

Support from the Swiss National Science Foundation to R.H. is gratefully acknowledged. This research was supported by a grant from the National Science Foundation (DMB-901250).

References

1 L. Stryer, Annu. Rev. Biochem., 47 (1978) 819.
2 K. Beardsley and C.R. Cantor, Proc. Natl. Acad. Sci. USA 65 (1970) 39.
3 C.H. Yang and D. Soll, Proc. Natl. Acad. Sci. USA 71 (1974) 2838.
4 J. Paoletti and J.B. Le Pecq, J. Mol. Biol. 59 (1971) 43.
5 J.L. Mergny, A. Slama-Schwok, T. Montenay-Garestier, M. Rougee and C. Hélène, Photochem. Photobiol. 53 (1991) 555.
6 B. Maliwal, J. Kusba and J.R. Lakowicz, SPIE Proc., Int. Soc. Opt. Eng. 1640 (1992) 586.
7 L.M. Smith, S. Fung, M.W. Hunkapiller, T.J. Hunkapiller and L.J. Hood, Nucleic Acids Res. 13 (1985) 2399.
8 S. Agrawal, C. Christodolou and M.J. Gait, Nucleic Acids Res. 14 (1986) 6227.
9 K.E. Gibson and S.J. Benkovic, Nucleic Acids Res. 15 (1987) 6455.
10 R.A. Cardullo, S. Agrawal, C. Flores, P.C. Zamenick and D.E. Wolf, Proc. Natl. Acad. Sci. USA 85 (1988) 8790.
11 J.P. Cooper and P.J. Hagerman, Biochemistry 29 (1990) 9261.
12 A.I.H. Murchie, R.M. Clegg, E. von Kitzing, D.R. Duckett, S. Diekmann and D.M.J. Lilley, Nature 341 (1989) 763.
13 S. Albaugh, J. Lan and R.F. Steiner, Biophys. Chem. 33 (1989) 71.
14 E. Haas, M. Wilchek, E. Katchalski-Katzir and I.Z. Steinberg, Proc. Natl. Acad. Sci. USA, 72 (1975) 2273.
15 S. Albaugh and R.F. Steiner, J. Phys. Chem. 93 (1989) 8013.
16 J.R. Lakowicz, M.L. Johson, W. Wiczk, A. Bhat and R.F. Steiner, Chem. PHys. Lett. 138 (1987) 587.
17 J.R. Lakowicz, J. Kusba, W. Wiczk, I. Gryczynski, H. Szmacinski and M.L. Johnson, Biophys. Chem. 39 (1991) 79.
18 J.R. Lakowicz, I. Gryczynski, H.C. Cheung, C.-K. Wang, M. L. Johnson and N. Joshi, Biochemistry 27 (1988) 9149.
19 J.R. Lakowicz, I. Gryczynski, W. Wiczk, G. Laczko, F.C. Prendergast and M.L. Johnson, Biophys. Chem. 36 (1990) 99.
20 P.R. Bevington, Data reduction and error analysis for the physical sciences, (McGraw-Hill, New York, 1969).
21 D. Holowa and B. Baird, Biochemistry 22 (1983) 3466.
22 E. Haas, E. Katchalski-Katzir and I.Z. Steinberg, Biochemistry 17 (1978) 5064.
23 A.J. Cross and G.R. Fleming, Biophys. J. 46 (1984) 45.
24 K. Kinosita, S. Kawato and A. Ikegami, Biophys. J. 20 (1977) 289.
25 W.H. Press, B.P. Flannery, S.A. Teukolsky and W.T. Vetterling, Numerical recipes (Cambridge University Press, New York, 1986).
26 D.P. Millar, R.A. Hochstrasser and S.M. Chen, SPIE Proc., Intl. Soc. Opt. Eng. 1640 (1992) 592.